Draft version January 8, 2014
Preprint typeset using LaTeX style emulateapj v. 11/12/01

arXiv:1401.1215v1 [astro-ph.GA] 6 Jan 2014

EXCITATION TEMPERATURE OF THE WARM NEUTRAL MEDIUM AS A NEW PROBE OF THE LYMAN-α RADIATION FIELD

Claire E. Murray[1], Robert R. Lindner[1], Snežana Stanimirović[1], W. M. Goss[2], Carl Heiles[3], John Dickey[4], Nickolas M. Pingel[1], Allen Lawrence[1], Jacob Jencson[2,5], Brian L. Babler[1], and Patrick Hennebelle[6],

Draft version January 8, 2014

ABSTRACT

We use the Karl G. Jansky Very Large Array (VLA) to conduct a high-sensitivity survey of neutral hydrogen (HI) absorption in the Milky Way. In combination with corresponding HI emission spectra obtained mostly with the Arecibo Observatory, we detect a widespread warm neutral medium (WNM) component with excitation temperature $\langle T_s \rangle = 7200^{+1800}_{-1200}$ K (68% confidence). This temperature lies above theoretical predictions based on collisional excitation alone, implying that Ly-α scattering, the most probable additional source of excitation, is more important in the interstellar medium (ISM) than previously assumed. Our results demonstrate that HI absorption can be used to constrain the Ly-α radiation field, a critical quantity for studying the energy balance in the ISM and intergalactic medium yet notoriously difficult to model because of its complicated radiative transfer, in and around galaxies nearby and at high redshift.

Subject headings: ISM: clouds — ISM: structure

1. INTRODUCTION

Understanding physical conditions within the diffuse neutral interstellar medium (ISM) is essential for producing realistic models of star and galaxy formation. Ambient gas temperature and density are crucial input parameters for heating, cooling and feedback recipes on all astronomical scales. While numerical simulations are becoming increasingly complex, details regarding neutral gas temperature distributions, shielding properties, essential feedback sources, and excitation processes are still very much under debate (Bryan 2007; Christensen et al. 2012). The excitation processes of the 21-cm line are especially important for interpreting radio signals from early epochs of cosmic structure formation (e.g., the cosmic dark ages and subsequent epoch of reionization), when neutral hydrogen dominated the baryonic content of the Universe and facilitated the formation of the first stars and galaxies (Pritchard & Loeb 2012). To interpret 21-cm signals from the early universe, it is necessary to decouple astrophysical effects from cosmological effects which is likely best done by analyzing excitation processes in the local ISM.

Traditional ISM models contain two neutral phases, the cold neutral medium (CNM) and the warm neutral medium (WNM), individually in thermal and pressure equilibrium (Field et al. 1969; McKee & Ostriker 1977; Wolfire et al. 2003). Widely-accepted theoretical properties of these phases in the Milky Way include: a kinetic temperature of $T_k \sim 40$–200 K and a volume density of $n(\mathrm{HI}) \sim 5$–$120\,\mathrm{cm}^{-3}$ for the CNM, and $T_k \sim 4100$–8800 K and $n(\mathrm{HI}) \sim 0.03$–$1.3\,\mathrm{cm}^{-3}$ for the WNM (Wolfire et al. 2003).

A convenient tracer for neutral gas is the HI 21-cm line, originating from the hyperfine energy splitting caused by magnetic moment interactions between the hydrogen atom's electron and proton. The high optical depth of the CNM makes 21-cm absorption signatures easy to detect, even with low sensitivity observations (e.g., Lazareff 1975; Dickey et al. 1977; Crovisier et al. 1978; Payne et al. 1978; Dickey et al. 1983; Braun & Walterbos 1992; Heiles & Troland 2003; Kanekar et al. 2003; Mohan et al. 2004; Roy et al. 2006; Begum et al. 2010). The excitation temperature (or spin temperature, T_s) of the CNM can be directly estimated by solving radiative transfer equations.

In contrast, the WNM is characterized by very-low peak optical depth and so measuring its spin temperature from absorption requires extremely high sensitivity, $\sigma_\tau \leq 10^{-3}$ and attention to systematic errors. Only two direct measurements of WNM spin temperature exist so far (Carilli et al. 1998; Dwarakanath et al. 2002). However, Carilli et al. (1998) observed absorption in the direction of Cygnus A, an exceptionally bright radio continuum source with a flux density of ~ 400 Jy, and achieved excellent sensitivity with orders of magnitude less integration time than is required for the majority of (> 3 Jy) radio continuum sources. Less accurate are upper limits on T_k (and thus T_s since $T_s \leq T_k$) estimated by spectral linewidths (Mebold et al. 1982; Kanekar et al. 2003; Heiles & Troland 2003; Roy et al. 2013b), and approximate T_s estimates obtained by assigning a single temperature to strongly-absorbing, complex HI profiles (Kanekar et al. 2011; Roy et al. 2013a).

Relating measured HI spin temperatures to model-predicted kinetic temperatures is further complicated by

[1] Department of Astronomy, University of Wisconsin, Madison, WI 53706, USA
[2] National Radio Astronomy Observatory, P.O. Box O, 1003 Lopezville, Socorro, NM 87801, USA
[3] Radio Astronomy Lab, UC Berkeley, 601 Campbell Hall, Berkeley, CA 94720, USA
[4] University of Tasmania, School of Maths and Physics,Private Bag 37, Hobart, TAS 7001, Australia
[5] Department of Astronomy, Ohio State University, 140 West 18th Avenue, Columbus, OH 43210
[6] Laboratoire AIM, Paris-Saclay, CEA/IRFU/SAp−CNRS− Université Paris Diderot, 91191 Gif-sur-Yvette Cedex, France

the uncertainty in the excitation mechanisms involved. The 21-cm transition in the high-density CNM is expected to be thermalized by collisions with electrons, ions, and other HI atoms, resulting in $T_s \sim T_k$. In contrast, low densities in the WNM imply that collisions cannot thermalize the 21-cm transition and therefore $T_s < T_k$ (Field 1958; Deguchi & Watson 1985; Liszt 2001). However, the Ly-α radiation field from Galactic and extragalactic sources can serve to thermalize the transition. This requires a very large optical depth and a large number of scatterings of Ly-α photons to bring the radiation field and the gas into local thermal equilibrium. While the underlying atomic physics is understood (Wouthuysen 1952; Field 1958; Pritchard & Loeb 2012), the details of Ly-α radiative transfer are complicated and depend on the topology and the strength of the Ly-α radiation field, which are complex and poorly constrained in the multi-phase ISM (Liszt 2001).

To measure the physical properties of the WNM and the coupling between neutral gas and Ly-α radiation, we are conducting a large survey, 21-cm Spectral Line Observations of Neutral Gas with the EVLA (21 SPONGE), to obtain high-sensitivity Milky Way HI absorption spectra using the Karl G. Jansky Very Large Array (VLA). The recently upgraded capabilities of the VLA allow us to routinely achieve RMS noise levels in optical depth of $\sigma_\tau \sim 7 \times 10^{-4}$ per 0.42 km s^{-1} channel, which are among the most sensitive observations of HI absorption to date. Currently, 24 out of 58 sightlines are complete after over 200 hours of observing time. This paper summarizes our initial results from this project and the detection of the WNM using a newly developed analysis technique based on the spectral stacking of HI absorption and emission spectra. In Section 2, we summarize our observing and data processing strategies, results of the stacking analysis are provided in Section 3 and discussed in Section 4, and we present our conclusions in Section 5.

2. OBSERVATIONS AND DATA PROCESSING

2.1. *Observations*

Each source, selected from the NRAO/VLA Sky Survey (Condon et al. 1998), was chosen to have a 1.4 GHz flux density ≥ 3 Jy to avoid excessively long integration times with the VLA to reach the desired sensitivity. In addition, we select sources generally at high Galactic latitude ($|b| > 10^\circ$) to avoid complicated CNM profiles associated with the Galactic plane, and with angular sizes less than $1'$ to avoid resolving substantial flux density. All VLA observations use three separate, standard L-band configurations, each with one dual-polarization intermediate frequency band of width 500 kHz with 256 channels, allowing for a velocity coverage of 107.5 km s^{-1} and resolution of 0.42 km s^{-1}. We perform bandpass calibration via frequency switching, and all data were reduced using the Astronomical Image Processing System[7] (AIPS). The absorption spectra, $\tau(v)$, were extracted from the final cleaned data cubes following calibration detailed in the 21 SPONGE pilot paper (Begum et al. 2010).

In addition, for each sightline we obtain HI emission profiles which estimate the brightness temperature ($T_{\rm B}(v)$) in the absence of the radio continuum source. Of our 24 sightlines, 11 have emission profiles from the Millennium Arecibo 21-cm Absorption Line Survey (Heiles & Troland 2003), 10 have emission profiles from the Galactic Arecibo L-band Feed Array Survey in HI (GALFA–HI; Stanimirović et al. 2006; Peek et al. 2011), and for 3 sightlines which were not included in the Millennium survey or the GALFA-HI survey to date, we use emission spectra from the Leiden Argentine Bonn (LAB; Kalberla et al. 2005) survey. Arecibo HI emission spectra have not been corrected for contamination entering the telescope beam through distant sidelobes (so called stray radiation).

[7] http://www.aips.nrao.edu

2.2. *Derivation of T_s for individual components*

To estimate T_s for individual spectral components, we follow the method of Heiles & Troland (2003). We first fit each absorption profile with Gaussian functions assuming thermal and turbulent broadening. We apply the statistical f-test to determine the best-fit number of components. We then fit the $T_{\rm B}(v)$ profile simultaneously for additional Gaussian components and T_s for each absorption-detected component by solving the radiative transfer equations discussed at length in Heiles & Troland (2003). These results will be presented along with additional survey information in Murray et al. 2014 (in prep).

We next construct "residual" spectra to search for weak absorption features below our observational sensitivity by removing fitted models from the absorption and emission profiles. The best-fitting Gaussian components in absorption ($\tau_i(v)$ where i denotes the $i^{\rm th}$ component) are subtracted from each original absorption profile $\tau(v)$ to produce a residual absorption spectrum, $\tau_{\rm res}(v) = \tau(v) - \Sigma\tau_i(v)$. The corresponding emission contribution from these components, $\Sigma T_{s,i}(1-e^{-\tau_i(v)})$, is removed from each emission profile, to produce a residual emission spectrum $T_{\rm B,res}(v) = T_{\rm B}(v) - \Sigma T_{s,i}(1-e^{-\tau_i(v)})$. Each residual emission spectrum is dominated by signals from the WNM purely detected in emission. Correspondingly, each residual absorption spectrum, $\tau_{res}(v)$, contains noise, model imperfections and weak absorption components below our detection threshold.

To minimize the effects of model imperfections in our results, we exclude sources from our analysis which have strong model-subtraction errors using the following technique. We first calculate the expected noise profile of the absorption spectrum, $\sigma_\tau(v)$, for each source. Because the LAB survey uses antennas of comparable size to those of the VLA, we follow methods described by Roy et al. (2013a) to estimate $\sigma_\tau(v)$ using LAB HI emission. We next produce probability distribution functions (PDFs) of $\tau_{res}(v)/\sigma_\tau(v)$ and exclude from further analysis 5/24 sources whose PDFs deviate from a normal distribution at $\geq 97.5\%$ confidence. The excluded sources are significantly contaminated by model-subtraction artifacts, and lie at low Galactic latitude where lines of sight probe many velocity-blended HI clouds, which complicates Gaussian modeling. Table 1 lists the source name, σ_τ calculated per 0.42 km s^{-1} velocity channel in offline channels, a weighting factor described in Section 3, and Galactic coordinates.

Table 1
Source Information

Name	σ_τ[a] ($\times 10^3$)	$W = 1/\sigma_\tau$[b] ($\times 10^2$)	l (deg)	b (deg)
4C32.44	1.5	2.7	67.240	81.049
4C25.43	0.9	4.5	22.464	80.991
3C286	0.7	5.8	56.527	80.676
4C12.50	1.3	3.1	347.220	70.173
3C273	0.6	6.7	289.945	64.358
3C298	0.8	5.1	352.159	60.667
3C225A	1.5	2.7	219.866	44.025
3C225B	3	1.3	220.010	44.007
3C345	1.3	3.1	63.455	40.948
3C327.1	1.4	2.9	12.181	37.006
3C147*	0.4	10.1	161.686	10.298
3C154*	0.9	4.5	185.594	4.006
3C410	1.9	2.1	69.210	−3.768
B2050+36*	2.3	1.8	78.858	−5.124
P0531+19	0.5	8.1	186.760	−7.110
3C111*	0.7	5.8	161.675	−8.821
3C133	1.8	2.2	177.725	−9.914
3C138	0.9	4.5	187.403	−11.347
3C123*	0.7	5.8	170.581	−11.662
3C120	1.1	3.7	190.373	−27.397
3C48	0.7	5.8	133.961	−28.720
4C16.09	0.8	5.1	166.633	−33.598
3C454.3	0.9	4.5	86.108	−38.182
3C78	4.1	1.0	174.857	−44.514

*Excluded sources (see Section 2.2).
[a]RMS noise in absorption profile calculated per 0.42 km s^{-1} channel.
[b]Normalized weighting factor (see Section 3); $\Sigma_n W_n = 1$.

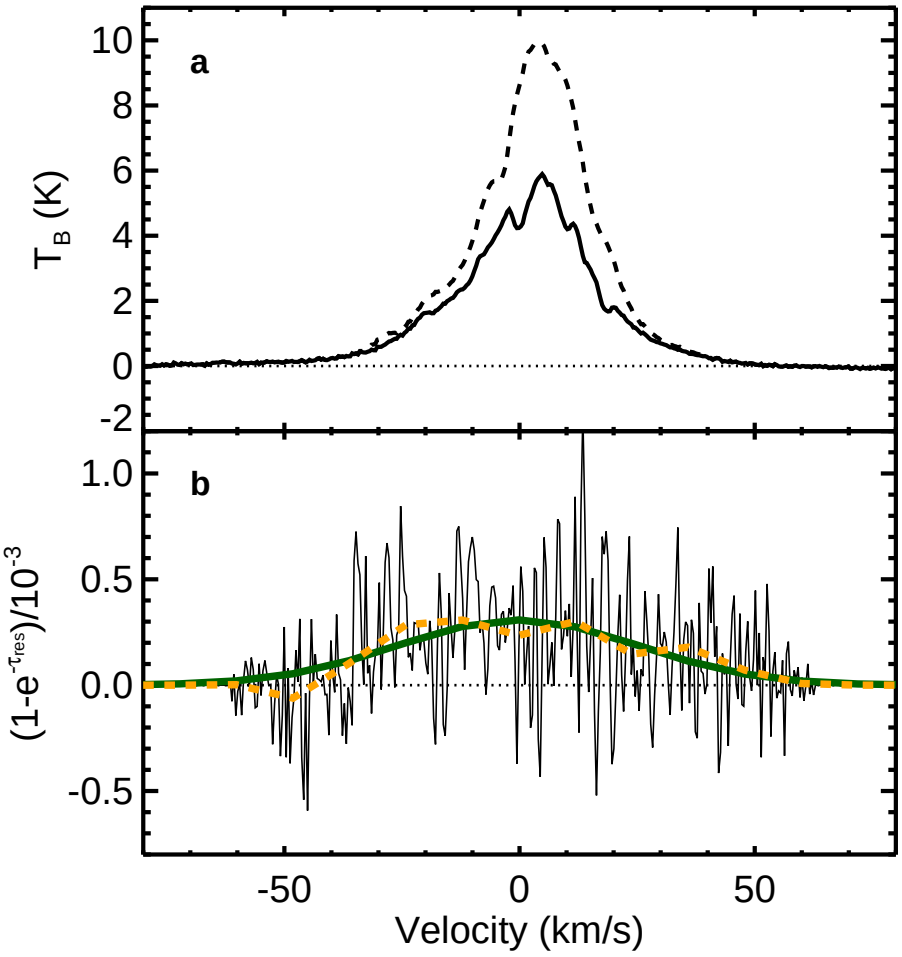

FIG. 1.— (**a**) The result of stacking the residual emission profiles $T_{\rm B,res}(v)$ (solid line) for the 19 selected sources, and the result of stacking the total emission profiles, $T_{\rm B}(v)$ (dashed line) for reference. (**b**) The result of stacking the residual VLA absorption profiles $\tau_{\rm res}(v)$ (thin solid black) from the selected 19 sources. A smoothed version of the stack ($10\,{\rm km\,s^{-1}}$ boxcar kernel) is overlaid (dashed orange), with a simple Gaussian fit to the profile overlaid (thick solid green). Due to the fact that all shifted profiles do not cover the same velocity range, we add zeroes to the edges of each profile so that they cover the same range. This results in fewer non-zero channels in the farthest velocity bins, which causes the noise level to be lower there.

3. STACKING ANALYSIS OF HI ABSORPTION AND EMISSION SPECTRA

We have performed a spectral "stacking" analysis on our 19 remaining residual spectra to search for extremely weak absorption signals from the diffuse WNM. We first apply a velocity shift to both the residual emission and absorption profiles to remove the effect of Galactic rotation and align any remaining signals at $0\,\mathrm{km\,s^{-1}}$. The velocity shifts are computed using the first velocity moment of the residual emission spectrum for each source, so that $\Delta v = -\int T_{\rm B,res}\, v\, dv / \int T_{\rm B,res} dv$. To maximize the signal to noise ratio of the stacked absorption spectrum, the weight, W, for each profile is given by $W = \tau_{\rm res}/\sigma_\tau^2$ (Treister et al. 2011). However, as discussed in the previous section, $\sigma_\tau \propto T_{\rm B}$. For constant T_s, we have $\tau_{\rm res} \propto T_{\rm B}$, and so the weight simplifies to: $W = 1/\sigma_\tau$. We measure σ_τ in the offline channels of each profile, and list these values with the weights W, normalized by the sum over all $n = 19$ profiles, $\Sigma_n W_n$, in Table 1. The same weighting values were applied to the residual emission spectra.

The weighted profiles are averaged to produce the final stacked emission and stacked absorption spectra shown in Figure 1. The RMS noise in the stacked absorption spectrum is $\sigma_\tau = 2.6 \times 10^{-4}$, calculated over a fixed range of channels (20 to 30 and -30 to -20 $\mathrm{km\,s^{-1}}$). This is 4.2 times more sensitive than the median RMS noise calculated in the same velocity channels in the individual residual absorption profiles ($\sigma_\tau = 1.15 \times 10^{-3}$).

The enhanced sensitivity enabled by stacking allows us to detect a weak and broad absorption component which has a velocity width and centroid consistent with the stacked *emission* signal (Figure 1). This gives confidence that the stacked profiles trace physically related quantities. This broad absorption component is the weighted-mean, $0\,\mathrm{km\,s^{-1}}$-centered absorption signal over all sightlines, and has an equivalent width (EW) within the velocity range common to all shifted profiles (-46 to $30\,\mathrm{km\,s^{-1}}$) of $\mathrm{EW} = \int_{-46}^{30}(1 - e^{-\tau_{\rm res}})dv = 0.018\,\mathrm{km\,s^{-1}}$.

We next conduct a bootstrapping (see, e.g., Wall & Jenkins 2003) Monte Carlo simulation to estimate the integrated strength of the stacked absorption signal (Figure 1b) and test for contamination by outlier spectra. We run the stacking analysis on a new sample of 19 sightlines randomly chosen from our original 19 sightlines with replacement. We repeat this trial 10^5 times, each time recomputing the EW. The resultant normalized PDF of EWs (Figure 2a, solid histogram) is nearly Gaussian, showing that the stacked EW signal is consistent with being drawn from a parent population of spectra with comparable means, and not due to a few outlier spectra. The peak of the EW distribution and the numerically-integrated 68% confidence limits are $\langle \mathrm{EW} \rangle = 0.0182^{+0.0044}_{-0.0036}\,\mathrm{km\,s^{-1}}$, giving 1 in 2×10^6 chance of being spurious (5σ). Figure 2a also displays the result of repeating the bootstrapping simulation while inverting (or multiplying by -1) a random selection of half of the profiles (dotted histogram). The result is fully consistent with zero signal, verifying that our stacking method does not produce spurious detections.

Using the Monte Carlo bootstrapping method, we also constrain the FWHM and peak optical depth of the stacked absorption feature by Gaussian fit as $\mathrm{FWHM} = 50^{+15}_{-7}\,\mathrm{km\,s^{-1}}$ and $\tau_0 = 3.0^{+1.0}_{-0.4} \times 10^{-4}$ (at the central velocity of the feature, v_0), respectively. Both quantities have well-defined, single-peaked distributions, suggesting that the detection is tracing a single gas component rather than a blend of many narrow components. We therefore proceed to estimate the typical spin temperature T_s of the gas detected in the stacked absorption spectrum.

We use three methods: (1) $T_s = \int_{-46}^{30} T_{\rm B,res}\, dv / \int_{-46}^{30}(1 - e^{-\tau_{\rm res}})\, dv$, (2) $T_s = T_{\rm B,res}(v_o)/(1 - e^{-\tau_{\rm res}})(v_o)$, where v_o is the velocity at the peak of the smoothed stacked absorption signal, and (3) by the methods of Heiles & Troland (2003), fitting a single Gaussian component to the absorption stack and solving for T_s by fitting this component to the emission stack without additional components. For each of the 10^5 bootstrapping trials, we compute all three T_s estimates and combine their distributions to minimize systematic errors associated with any individual approach (Figure 2b).

We estimate a spin temperature of the detected absorption feature of $\langle T_s \rangle = 7200^{+1800}_{-1200}\,\mathrm{K}$ (68% confidence), with a lower limit at 99% confidence of 4300 K. We note that by shifting the residual profiles by the second velocity moment or by the location of maximum $T_{\rm B,res}$, we find consistent temperature estimates with similar significance. The possible contamination of stray radiation to the Arecibo HI emission spectra has no effect on the presence of the absorption stack, although it will tend to increase the EW of the emission stack, and therefore increase the estimated T_s of the stacked feature. For the GALFA-HI survey, Peek et al. (2011) estimated that the level of stray radiation contamination is $\leq$ 200–500 mK, leading to an overestimate in our computed T_s of at most 13%. Therefore, the presence of stray radiation in our Arecibo HI emission spectra would not change our results

4. DISCUSSION

In Figure 3, we plot all previous WNM T_s detections (open symbols) against the RMS noise in off-line channels of the individual absorption spectra in which they were detected, with 1σ error bars derived from line fitting. We exclude literature measurements which are estimated as upper limits from T_k or which assume single temperatures for multi-component sightlines. Our result from the stacking analysis (green filled star) is in agreement with measurements by Carilli et al. (1998) (open triangles) obtained in the direction of ~ 400 Jy-bright Cygnus A. We emphasize that our result samples a widespread population detected from 19 sightlines, while Carilli et al. (1998) examine only a single direction. Our T_s estimate is significantly higher than all other direct measurements shown here. The trend of increasing T_s with increasing observational sensitivity confirms the expectation that previous experiments with lower sensitivity ($\sigma_\tau \geq 5 \times 10^{-4}$) were unable to detect WNM with $T_s > 1000\,\mathrm{K}$ due to its low optical depth.

The range of predicted *kinetic* temperatures from the most detailed ISM heating and cooling considerations, shown by the dotted purple hatched region in Figure 3, is $T_k \sim 4100$–$8800\,\mathrm{K}$ (Wolfire et al. 2003). We use models considering only collisional excitation from Liszt (2001) (their Figure 2) to show that under all plausible ISM

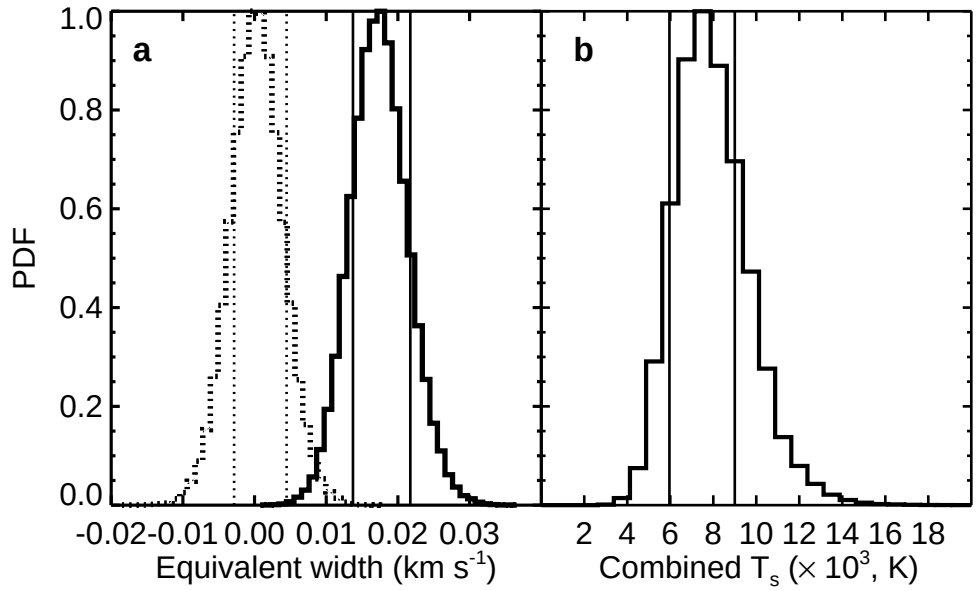

FIG. 2.— (**a**) PDF of stacked absorption EW following 10^5 iterations using a bootstrapping algorithm to select 19 sources from the total list of 19 with replacement, yielding $\langle \mathrm{EW} \rangle = 0.0182^{+0.0044}_{-0.0036}$ km s^{-1} (68% confidence). To test that the signal is real, we invert (or multiply by -1) a random selection of half of the absorption residual profiles in 10^5 additional trials, yielding a distribution (dotted histogram) consistent with zero signal, as expected. Vertical lines denote 1σ uncertainty limits. (**b**) Distribution of spin temperatures from combining the PDFs of three different estimations (see text) computed in all 10^5 bootstrapping trials. The derived spin temperature is $\langle T_s \rangle = 7200^{+1800}_{-1200}$ K (68% confidence), with a 99% confidence lower limit of 4300 K.

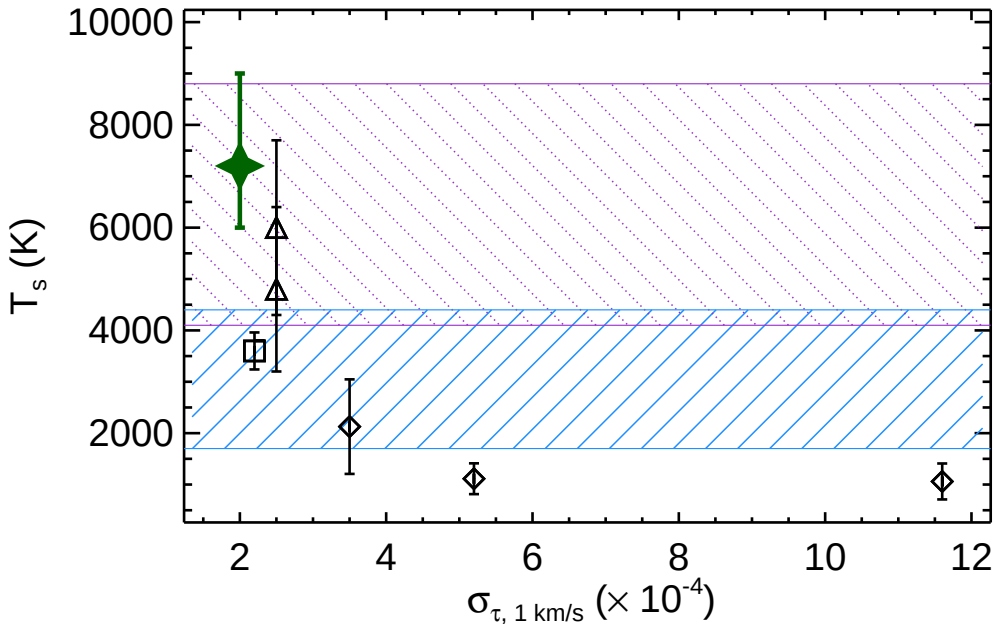

FIG. 3.— Comparison of previous T_s measurements for the WNM. Hollow symbols denote direct observational measurements of individual sightline components. *Triangles*: Absorption towards Cygnus A (Carilli et al. 1998), *Square*: Absorption towards 3C147 (Dwarakanath et al. 2002) *Diamonds*: 21 SPONGE absorption towards PKS0531+19, 3C298 and 3C133. All points are plotted versus the RMS noise in off-line channels in the absorption profile, per 1km s^{-1} channel ($\sigma_{\tau,1\mathrm{km/s}}$). The purple dotted hatched region denotes the *kinetic* temperature range from Wolfire et al. (2003) ($T_k \sim$ 4100–8800 K), and the blue hatched region denotes the *spin* temperature range from Liszt (2001) for all possbile ISM pressures ($T_s \sim$ 1800–4400 K). The green filled star is the derived spin temperature from Figure 2b, $\langle T_s \rangle = 7200^{+1800}_{-1200}$ K (68% confidence), with a 99% confidence lower limit of 4300 K.

pressures, the range of spin temperatures implied by this T_k range from Wolfire et al. (2003), is $T_s \sim 1800$–$4400\,\mathrm{K}$ (solid blue hatched region in Figure 3). Our measurement indicates that the mean spin temperature of the WNM is higher than expected theoretically for collisionally excited HI at 98% confidence.

Resonant scattering of Ly-α photons can contribute enough to 21-cm excitation to allow $T_s = T_k$, as long as a sufficient fraction of the Ly-α radiation permeates the WNM (Liszt 2001; Pritchard & Loeb 2012). However, the degree to which this can occur in a multi-phase ISM depends on several observationally unconstrained quantities: the local and external Ly-α field, interstellar pressure, interstellar turbulence, ionization fraction, and the topology of the ISM. Using models from Liszt (2001), which assume a column density of hydrogen nuclei equal to $10^{19}\,\mathrm{cm}^{-2}$ and the temperature of the Ly-α radiation field being equal to the kinetic temperature, our T_s measurement constrains the fraction of Galactic flux from early-type stars which permeates HI clouds to $> 1 \times 10^{-4}$.

Our work provides the first observational evidence for the Ly-α mechanism acting throughout the bulk of the Galactic WNM. By increasing observational sensitivity to T_s in comparison with expectations for T_k, stacking can be used to constrain the importance of non-collisional excitation on HI, as well as the origin and intensity of the Ly-α radiation field. In the future, 21 SPONGE will obtain more absorption sightlines to increase our sensitivity to weak underlying signatures of the WNM, thereby further refining these temperature constraints, and sampling different Galactic environments.

5. CONCLUSIONS

We have presented the discovery of a weak ($\tau_0 = 3.0^{+1.0}_{-0.4} \times 10^{-4}$), broad (FWHM $= 50^{+15}_{-7}\,\mathrm{km\,s^{-1}}$) WNM absorption feature in the stacked absorption spectrum of 19 independent Galactic sight-lines from the 21-SPONGE survey. Using Monte Carlo simulations, we have estimated the feature's spin temperature to be $\langle T_s \rangle = 7200^{+1800}_{-1200}\,\mathrm{K}$, which is significantly (98% confidence) higher than theoretical predictions based on collisional excitation alone, likely due to the thermalization of HI by resonant Ly-α scattering. This work provides the first observational evidence that the Ly-α excitation mechanism is acting throughout the bulk of the Galactic WNM, and demonstrates that the Ly-α radiation field, a quantity that is difficult to measure yet vitally important for interpreting HI signals from early epochs of cosmic structure formation, can be probed using measurements of the WNM.

We thank an anonymous referee for helpful comments and suggestions. This work was supported by the NSF Early Career Development (CAREER) Award AST-1056780. C. M. acknowledges support by the National Science Foundation Graduate Research Fellowship and the Wisconsin Space Grant Institution. S. S. thanks the Research Corporation for Science Advancement for their support. We thank A. Begum for help with initial survey observations, D. Able for developing initial data reduction strategy, and H. Liszt, J. S. Gallagher, N. Roy and T. Wong for helpful discussions. The National Radio Astronomy Observatory is a facility of the National Science Foundation operated under cooperative agreement by Associated Universities, Inc. The Arecibo Observatory is operated by SRI International under a cooperative agreement with the National Science Foundation (AST-1100968), and in alliance with Ana G. Méndez-Universidad Metropolitana, and the Universities Space Research Association.

REFERENCES

Begum, A., Stanimirović, S., Goss, W., et al. 2010, ApJ, 725, 1779
Braun, R., & Walterbos, R. A. M. 1992, ApJ, 386, 120
Bryan, G. 2007, in EAS Publications Series, Vol. 24, EAS Publications Series, ed. E. Emsellem, H. Wozniak, G. Massacrier, J.-F. Gonzalez, J. Devriendt, & N. Champavert, 77–88
Carilli, C. L., Dwarakanath, K. S., & Goss, W. M. 1998, ApJ, 502, L79
Christensen, C., Quinn, T., Governato, F., et al. 2012, MNRAS, 425, 3058
Condon, J., Cotton, W., Greisen, E., et al. 1998, AJ, 115, 1693
Crovisier, J., Kazes, I., & Aubry, D. 1978, A&AS, 32, 205
Davies, R. D., & Cummings, E. R. 1975, MNRAS, 170, 95
Deguchi, S., & Watson, W. D. 1985, ApJ, 290, 578
Dickey, J., Kulkarni, S., van Gorkom, J., & Heiles, C. 1983, ApJS, 53, 591
Dickey, J. M., Salpeter, E. E., & Terzian, Y. 1977, ApJ, 211, L77
Dwarakanath, K. S., Carilli, C. L., & Goss, W. M. 2002, ApJ, 567, 940
Field, G. B. 1958, Proceedings of the IRE, 46, 240
Field, G. B., Goldsmith, D. W., & Habing, H. J. 1969, ApJ, 155, L149
Heiles, C., & Troland, T. 2003, ApJS, 145, 329
Kalberla, P., Burton, W., Hartmann, D., et al. 2005, A&A, 440, 775
Kanekar, N., Braun, R., & Roy, N. 2011, ApJ, 737, L33
Kanekar, N., Subrahmanyan, R., Chengalur, J. N., & Safouris, V. 2003, MNRAS, 346, L57
Lazareff, B. 1975, A&A, 42, 25
Liszt, H. 2001, A&A, 371, 698
McKee, C., & Ostriker, J. 1977, ApJ, 218, 148
Mebold, U., Winnberg, A., Kalberla, P. M. W., & Goss, W. M. 1982, A&A, 115, 223
Mohan, R., Dwarakanath, K., & Srinivasan, G. 2004, Journal of Astrophysics and Astronomy, 25, 143
Payne, H., Dickey, J., Salpeter, E., & Terzian, Y. 1978, ApJ, 221, L95
Peek, J., Heiles, C., Douglas, K., et al. 2011, ApJS, 194, 20
Pritchard, J. R., & Loeb, A. 2012, Reports on Progress in Physics, 75, 086901
Roy, N., Chengalur, J. N., & Srianand, R. 2006, MNRAS, 365, L1
Roy, N., Kanekar, N., Braun, R., & Chengalur, J. 2013a, ArXiv e-prints, 1309.4098
Roy, N., Kanekar, N., & Chengalur, J. 2013b, ArXiv e-prints, arXiv:1309.4099
Stanimirović, S., Putman, M., Heiles, C., et al. 2006, ApJ, 653, 1210
Treister, E., Schawinski, K., Volonteri, M., Natarajan, P., & Gawiser, E. 2011, Nature, 474, 356
Wall, J. V., & Jenkins, C. R. 2003, Practical Statistics for Astronomers (Cambridge University Press)
Wolfire, M., McKee, C., Hollenbach, D., & Tielens, A. 2003, ApJ, 587, 278
Wouthuysen, S. A. 1952, AJ, 57, 31